IJC Heart & Vasculature 32 (2021) 100703

Contents lists available at ScienceDirect

IJC Heart & Vasculature

journal homepage: www.journals.elsevier.com/ijc-heart-and-vasculature

Characterization of left ventricular cavity flow, wall stress and energy loss by color doppler vector flow mapping in children and adolescents with cardiomyopathy

Mary Craft [a], Vivek Jani [b], John Bliamptis [b], Benjamin T Barnes [b], Christopher C Erickson [a], Andreas Schuster [c], David A Danford [a], Shelby Kutty [b,*]

[a] Dr. C.C. and Mabel L. Criss Heart Center, University of Nebraska College of Medicine and Children's Hospital and Medical Center, Omaha, NE, USA
[b] Helen B. Taussig Heart Center, Department of Pediatrics, Johns Hopkins Hospital, Baltimore, MD 21205-2196, USA
[c] Department of Cardiology and Pneumology, University Medical Center Göttingen Georg-August University Göttingen Germany

ARTICLE INFO

Article history:
Received 1 December 2020
Accepted 7 December 2020

Keywords:
Diastolic function
Echocardiography
Vector flow mapping
Hypertrophic cardiomyopathy
Dilated cardiomyopathy

ABSTRACT

Background: Vector flow mapping is an emerging echocardiographic method allowing for investigation of intracardiac blood flow mechanics, wall shear stress (WSS), and energy loss (EL). We hypothesized that alterations in EL and WSS will differ among subjects with hypertrophic (HCM), dilated (DCM) cardiomyopathy, and normal controls.

Methods: Echocardiograms were prospectively performed with the ProSound F75CV (Hitachi HealthCare., Tokyo, Japan) on all subjects. 2D color Doppler cine loop images were obtained from apical 5 and the apical long axis views and stored digitally. Measurements were averaged over three cardiac cycles using VFM software to derive flow patterns, WSS, and EL. Standard left ventricular (LV) systolic and diastolic functional parameters were also obtained.

Results: A total of 85 subjects, 22 with HCM (age 18 ± 9 yrs.), 18 DCM (age 18 ± 9 yrs.), and 45 age and gender matched controls were included in the study. Diastolic wall shear stress was found significantly different in HCM (0.004 ± 0.185 N/m^2) compared with DCM (0.397 ± 0.301 N/m^2, $P < 0.001$), and controls (0.175 ± 0.255 N/m^2, $P = 0.027$). Furthermore, indexed systolic EL was found to be significantly elevated in HCM (13.91 ± 13.17 $mW/m^2/m^3$) compared with DCM (8.17 ± 9.77 $mW/m^2/m^3$, $P < 0.001$), but not controls (6.45 ± 7.47 $mW/m^2/m^3$).

Conclusion: Differences in abnormal ventricular mechanics observed in HCM and DCM are reflected in both EL and WSS, and are suggestive that changes in energetic parameters may represent novel indices of ventricular dysfunction.

1. Introduction

Vector flow mapping (VFM) is an emerging echocardiographic method which processes Doppler color flow maps to calculate velocity vectors and thereby demonstrate intracardiac blood flow mechanics [1]. The algorithm extracts information from the distribution of color flow Doppler, estimates the radial component of the flow distribution, and then displays it without angle dependence [1]. The ventricular remodeling processes associated with cardiomyopathy alter the left ventricular (LV) hemodynamics which includes the energy loss (EL), which is the frictional heat generated by the viscosity of the blood), within the ventricle. The intracardiac EL can be derived from vector mapping flow (VFM) using the viscosity of the blood ($\mu = 4$ centipoise) and the two-dimensional velocity vector component along the Cartesian coordinate. EL describes the total of the squared differences between neighboring velocity vectors and is becoming the new hemodynamic index for assessing cardiac function [2]. Energy change in the blood of the LV likely consists of two components: (1) transfer of kinetic energy from the blood to the LV wall, which is necessary for effective cardiac function, and (2) EL due to friction and heat generation associated with vortices. To be energy efficient, the transfer of kinetic energy needs to take place with a minimum of EL. We hypothesize that the left ventricle in both dilated cardiomyopathy (DCM) and hypertrophic cardiomyopathy (HCM) are energy inefficient relative to normal, but likely due to different mechanisms. The purpose of this investigation is to use VFM to test the hypothesis that patterns

* Corresponding author.
E-mail address: skutty1@jhmi.edu (S. Kutty).

https://doi.org/10.1016/j.ijcha.2020.100703
2352-9067/

of EL in the LV differ among subjects with HCM, DCM, and normal controls.

2. Methods

This was a single center prospective study of 85 subjects aged 0–40 years, including with LV cardiomyopathy (22 with HCM, 18 with DCM), and 45 healthy controls. The cardiomyopathy group was recruited from the population of patients followed at Children's Hospital and Medical Center, and their relatives less than or equal to 40 years old with the same cardiac condition. Patients with ECG abnormalities, including bundle branch block, were excluded. Healthy age and gender matched volunteers with no known history of heart disease, cardiomyopathy, or relevant comorbidities and with normal cardiac function served as controls. The study was approved by the institutional review board, with written informed consent required from all participants. Subjects unable to remain still long enough for the image acquisition or unable to provide a written informed consent were excluded from the study. Review of the subjects' medical records provided clinical and demographic data including age, gender, height, weight, body surface area (BSA), blood pressure, heart rate, and cardiac diagnosis.

2.1. Image acquisition

Echocardiograms were prospectively performed with the ProSound F75CV (Hitachi HealthCare., Tokyo, Japan) with the UST-52105 (1.8–2.5 MHz) probe on all subjects, by an experienced sonographer. All subjects were examined in the left lateral decubitus position. 2D color Doppler cine loop images were obtained from apical 5 and apical long axis views and stored digitally. The apical long axis view was utilized for analysis due to its superior alignment. The Nyquist limit was set high enough to minimize aliasing. The imaging depth, sector size, and spatial–temporal settings were set to obtain the highest frame rates while including the entire left ventricle, mitral and aortic valves in the color scan area. Color frame rate range was 30–55 frames/sec. End-diastolic and end-systolic LV volumes, indexed LA volumes, stroke volume (SV), and ejection fraction (EF) were calculated using the biplane Simpson's method. Cardiac output was obtained as the product of the stroke volume and heart rate, and divided by BSA to yield cardiac index (CI). Transmitral Doppler flow was recorded in apical four-chamber view (A4C) by placing the sample volume at the tip of the mitral leaflets to measure early filling peak (E) wave and late filling peak (A) wave velocities, from which the E/A ratio was calculated. The peak e' and a' wave were measured by tissue Doppler imaging of the lateral and septal wall in the A4C view. E/e' was calculated as a surrogate for LV filling pressure or LV diastolic function [3,4]. Global longitudinal and circumferential strain (GLS and GCS) were measured [5,6].

2.2. Analysis of LV strain, strain rate, energy loss, and wall shear stress

2D transthoracic echocardiographic analyses were performed using commercially available software (DAS-RS1, Hitachi HealthCare., Tokyo, Japan) to evaluate LV GLS, GCS, and strain rate. The LV parasternal short axis at mid papillary level and the A4C views were recorded using conventional 2D grayscale imaging. The 2D frame rate was set to at least 50–60 frames/second for all views. The LV endocardial border was manually delineated, and the software automatically tracked the contours on the other frames. The region of interest (ROI) was depicted. The software automatically generated curves of the LV GLS, GCS, and strain rate. Fig. 1 shows a representation of VFM software utilized for analysis.

EL, expressed as friction energy due to blood viscosity, was calculated from velocity vector components. The 2D color Doppler LV cine loop images in the apical long axis view were analyzed with the VFM software. The heart rate (HR) was calculated based on the RR interval of the cardiac cycle, which was divided into two phases: ventricular systole, and ventricular diastole. The LV endocardial border was manually traced and pre-processed with the ROI drawn to incorporate the entire LV, the distribution of EL could be displayed in two dimensions. Calculations of EL were made from frame-by-frame velocity vector fields of the cine-loop. Measurements in both systole and diastole were averaged over 3 cardiac cycles. The efficiency with which the LV can generate output relative to the energy loss within it was estimated by SV/EL.

The VFM software also provided measurements of the wall shear stress (WSS) around the LV wall boundary, and this was measured in both systole and diastole [7]. Since WSS is proportional to the velocity gradient in normal direction, the velocity gradient value is obtained and displayed in color. To measure WSS, an apical long axis view was obtained, and the ROI was drawn to incorporate the entire LV. The VFM meshes were not boundary-fitted but, instead, fixed in a measurement plane. The velocity at a point one pixel away from the wall was used, the element that included the point was identified, and the velocity vector component parallel to the wall was interpolated. WSS was calculated using the first differential between this velocity and the speckle-tracking measured wall velocity [7]. Each frame was captured as a CSV file. Calculation of WSS was made from frame-by-frame velocity vector fields of the cine-loop and WSS was averaged for each frame. Measurements were averaged over 3 cardiac cycles and the following measurements were made: WSS diastolic average, systolic average, diastolic average maximum, and systolic average maximum.

2.3. Statistical analysis

Continuous data were summarized using means (standard deviations). Analysis of Variance (ANOVA) was used to compare differences in continuous variables among the three groups (HCM, DCM and Control) when all assumptions were met. When ANOVA suggested significant variation, pairwise comparisons were made between groups with Bonferroni correction for multiple comparisons. Pearson correlation coefficient was used to assess associations amongst the variables. Results were considered statistically significant for p-values < 0.05. SAS v9.4 (SAS institute, Cary, NC) was used for all computations.

3. Results

3.1. Participant demographic characteristics and echocardiographic parameters

A total of 85 subjects, 22 with HCM (age 18 ± 9 yrs.), 18 DCM (age 18 ± 9 yrs.), and 45 age and gender matched controls were included in the study. Demographic features and echocardiographic parameters are summarized in Table 1. Significant differences were observed in biplane ejection fraction, E/e', left atrial volume index, and ventricular strain between groups. Ejection fraction was observed to be significantly depressed in DCM compared to both controls ($P < 0.001$) and HCM ($P < 0.001$). E/e' was found to be significantly elevated in both HCM ($P < 0.0001$) and DCM ($P < 0.001$) compared to controls. Furthermore, left atrial volume index was observed to be elevated in HCM ($P = 0.023$) compared to controls. GLS and GCS were observed to be significantly depressed in DCM compared to HCM (GLS – $P = 0.023$; GCS - $P < 0.001$) and controls (GLS – $P < 0.001$; GCS - $P < 0.001$). No sig-

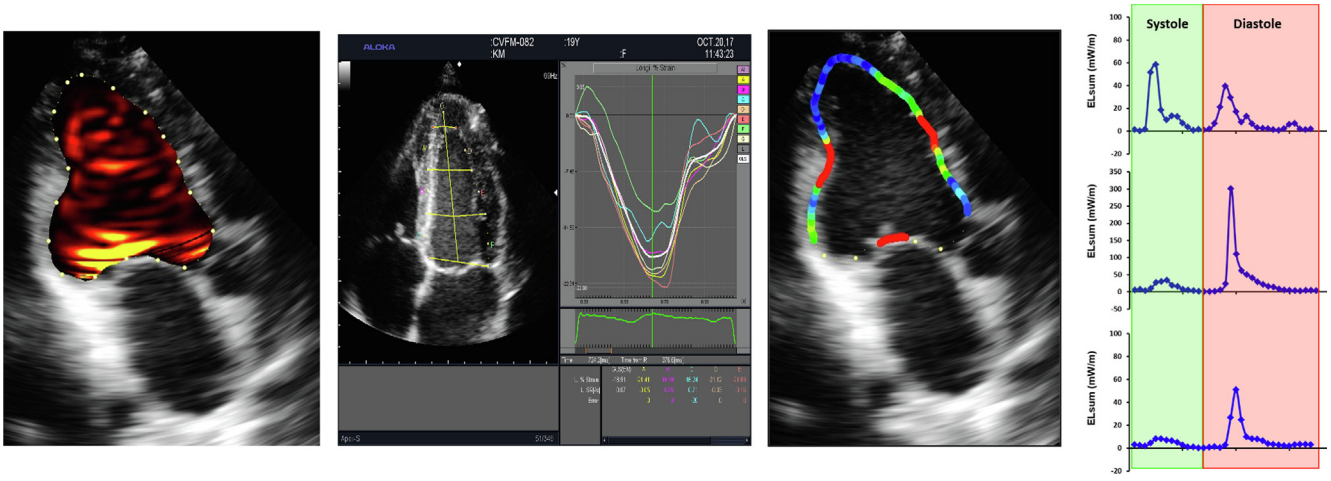

Fig. 1. Representation of Vector Flow Mapping software utilized for determination of energy loss, global longitudinal strain, and wall shear stress. From left to right, energy loss (left) during the cardiac cycle determined utilizing vector flow mapping, global longitudinal strain, and wall shear stress from vector flow mapping were determined for all patients using the DAS-RS1, Hitachi HealthCare software. A representative trace of calculated energy loss over the cardiac cycle is shown on the right.

Table 1
Demographic Features and Echocardiographic Parameters by Group.

	HCM (N = 22)	DCM (N = 18)	Control (N = 45)	P Value (ANOVA)
Age (yrs)	18.17 ± 9.48	18.44 ± 8.6	18.36 ± 8.74	0.995
BSA (m^2)	1.80 ± 0.66	1.65 ± 0.57	1.67 ± 0.52	0.637
HR (bpm)	70.82 ± 17.0	81.39 ± 23.7	68.93 ± 16.7	0.055
SV (mL)	63.69 ± 25.47	50.63 ± 24.63	60.36 ± 22.59	0.206
Biplane EF (%)	63.36 ± 5.60	41.22 ± 14.1	62.09 ± 3.94	**< 0.0001**
CI(L/min/m2)	2.34 ± 0.58	2.47 ± 0.81	2.44 ± 0.57	0.792
E/A	1.56 ± 0.49	1.91 ± 1.0	1.98 ± 0.60	0.061
E/e'	7.26 ± 2.4	6.85 ± 3.3	4.06 ± 1.1	**< 0.0001**
LA Vol Index (mL/m2)	28.36 ± 11.8	28.02 ± 15.3	22.18 ± 5.8	0.027
Longitudinal Strain	−14.88 ± 3.2	−11.49 ± 4.0	−18.89 ± 2.0	**< 0.0001**
Circumferential Strain	−25.73 ± 5.9	−12.36 ± 6.0	−24.99 ± 3.1	**< 0.0001**

BSA – Body Surface Area, HR – Heart Rate, SV – Stroke Volume, EF – Ejection Fraction, CI – Cardiac Index, LA Vol Index – Left Atrial Volume Index.

nificant differences were observed in the remaining demographic features and echocardiographic parameters.

3.2. Energetic parameters

Table 2 summarizes energetic parameters, namely average and maximum WSS during systole and diastole, and total, systolic, and diastolic EL over one and three cycles in controls, HCM, and DCM. Of all energetic parameters considered, significant differences were observed in average and maximum diastolic WSS and systolic EL between all groups. Briefly, average diastolic WSS was significantly decreased in HCM compared with DCM ($P < 0.001$) and controls ($P = 0.027$); however average diastolic WSS was significantly elevated in DCM compared with controls ($P = 0.005$). While a similar trend was observed for maximum diastolic WSS, a significant difference was only observed between HCM and DCM ($P = 0.023$). In addition, maximum systolic WSS was observed to be significantly elevated in HCM compared with DCM ($P = 0.028$).

Changes in intracardiac EL associated with kinetic energy transfer and friction losses from intracardiac vortices were calculated during both systole and diastole and averaged over 3 cardiac cycles (Table 2). Strikingly, no significant differences were observed in total EL and diastolic EL between HCM, DCM, and controls. However, indexed systolic EL was observed to be significantly elevated in HCM relative to controls ($P = 0.012$). While no significant differences were observed between DCM and controls, indexed systolic EL was observed to be significantly elevated in HCM compared with DCM ($P < 0.001$). Fig. 2 graphically depicts changes in indexed total, systolic, and diastolic EL. The remaining statistical analysis is presented in Table 2.

3.3. Univariate correlations between energetic parameters and other covariates

Univariate correlations and multivariate regressions were performed for energetic parameters, namely systolic and energetic WSS and systolic and diastolic EL, and relevant demographic and echocardiographic data, for all patients, controls, HCM, and DCM in the study. Diastolic WSS demonstrated significant correlations with age, heart rate, biplane EF, E/A ratio, and GCS. A similar finding was observed for EL parameters. The total EL, systolic EL, and diastolic EL demonstrated significant correlations with age, BSA, HR, CI, and E/e'. These results are summarized in Table 3 for all patients and Supplemental Table 1 for controls. Multivariate regression, presented in **Supplemental** Tables 2 and 3 of energetic parameters and echocardiographic covariates, yielded similar findings. Briefly, significant correlations were observed between all EL parameters and HR. Furthermore, indexed total EL and indexed systolic EL demonstrated significant correlations with E/e'. No significant correlations were observed between WSS and most EL parameters and ventricular strain parameters.

4. Discussion

Abnormal systolic and diastolic ventricular mechanics are known to adversely influence ventricular fluid mechanics in both

Table 2
Energetic Parameters. Pairwise comparisons were performed for all results with P < 0.05 from one-way ANOVA and are summarized below. Average WSS – Diastolic. Control vs. DCM P = 0.005; HCM vs. DCM P < 0.001; Control vs. HCM P = 0.027. Max WSS – Diastolic. Control vs. DCM P = 0.225; HCM vs. DCM P = 0.028; Control vs. HCM P = 0.576. Max WSS – Systolic. Control vs. DCM P = 0.950; HCM vs. DCM P = 0.023; Control vs. HCM P = 0.079. 1 cycle EL – Systolic ($mW/m^2/m^3$). Control vs. DCM P = 1.000; HCM vs. DCM P < 0.001; Control vs. HCM P < 0.001. 1 cycle Indexed EL – Systolic ($mW/m^2/m^3$). Control vs. DCM P = 1.000; HCM vs. DCM P = 0.200; Control vs. HCM P = 0.012. 3 cycle EL – Systolic ($mW/m^2/m^3$). Control vs. DCM P = 0.695; HCM vs. DCM P = 0.011; Control vs. HCM P < 0.001. 3 cycle indexed EL – Systolic ($mW/m^2/m^3$). Control vs. DCM P = 0.614; HCM vs. DCM P < 0.001; Control vs. HCM P = 0.012.

	HCM (N = 22)	DCM (N = 18)	Control (N = 45)	P Value (ANOVA)
Wall Shear Stress (WSS)				
Average WSS – Systolic (N/m^2)	0.39 ± 0.23	0.36 ± 0.26	0.41 ± 0.13	0.754
Max WSS – Systolic (N/m^2)	1.01 ± 0.47	0.71 ± 0.40	0.81 ± 0.22	**0.019**
Average WSS – Diastolic (N/m^2)	0.004 ± 0.185	0.40 ± 0.30	0.18 ± 0.26	**< 0.0001**
Max WSS – Diastolic (N/m^2)	0.52 ± 0.35	0.88 ± 0.55	0.66 ± 0.41	**0.033**
Energy Loss (EL) – 1 Cycle				
Total EL (mW/m^3)	22.42 ± 15.52	17.62 ± 11.96	17.48 ± 11.17	0.296
Indexed Total EL ($mW/m^2/m^3$)	19.22 ± 33.67	14.72 ± 16.54	14.04 ± 17.65	0.671
EL – Systolic (mW/m^3)	19.35 ± 9.99	9.76 ± 7.95	8.17 ± 4.88	**< 0.0001**
Indexed EL – Systolic ($mW/m^2/m^3$)	13.91 ± 13.17	8.17 ± 9.77	6.45 ± 7.47	**0.015**
EL – Diastolic (mW/m^3)	27.36 ± 17.93	25.79 ± 17.93	25.96 ± 20.96	0.971
Indexed EL – Diastolic ($mW/m^2/m^3$)	28.19 ± 72.65	22.12 ± 26.59	21.90 ± 34.18	0.862
Energy Loss (EL) – 3 Cycles				
Total EL (mW/m^3)	22.59 ± 16.42	19.38 ± 12.89	17.29 ± 10.40	0.280
Indexed Total EL ($mW/m^2/m^3$)	18.79 ± 30.06	15.58 ± 16.35	13.80 ± 16.91	0.660
EL – Systolic (mW/m^3)	17.06 ± 10.46	10.35 ± 7.48	7.98 ± 4.10	**< 0.0001**
Indexed EL – Systolic ($mW/m^2/m^3$)	12.02 ± 11.06	8.68 ± 10.19	5.81 ± 4.76	**0.014**
EL – Diastolic (mW/m^3)	29.76 ± 31.90	38.73 ± 20.18	25.54 ± 18.93	0.763
Indexed EL – Diastolic ($mW/m^2/m^3$)	28.82 ± 64.92	22.95 ± 25.16	21.87 ± 34.22	0.820

Energy Loss normalized to Stroke Volume.

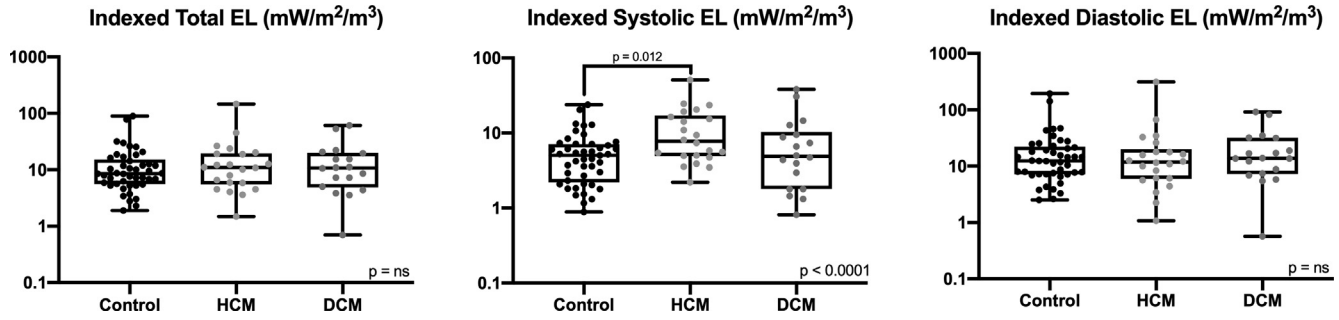

Fig. 2. Indexed total (left), systolic (middle), and diastolic (right) energy loss (EL) in Controls, HCM, and DCM. Significant differences between all groups were observed for indexed systolic energy loss (P < 0.0001).

adult and pediatric populations [8–10]. Traditionally, changes in systolic EL reflect changes in cardiac contractility, while changes in WSS reflect dysfunction at the level of the ventricular endocardium [7,9]. Recent data suggests that changes in ventricular EL may represent a novel index of ventricular dysfunction with potential as a cardiovascular outcomes predictor [11]. Utilizing VFM, a well-established echocardiographic method for quantification of ventricular velocity and vorticity profiles [9,12,13], this study quantified both systolic and diastolic ventricular WSS and intracardiac EL in HCM and DCM and correlated these data with traditional echocardiographic parameters. Our study demonstrated significant elevation in diastolic WSS and indexed systolic EL in HCM. Few differences were observed in energetic parameters in DCM. Furthermore, weak correlations between WSS and EL parameters between age, HR, E/A, and E/e' support what has been previously reported in the literature [9,10,12]. Our findings suggest that changes in energetic parameters may represent novel indices of ventricular diastolic dysfunction.

Intracardiac EL is a measure of the efficiency of ventricular blood flow and vortex formation, which is required for efficient systolic ejection [9,12,14–16]. In the healthy human LV, a large basilar vortex during systole is sustained throughout the entirety of isovolumic contraction and immediately dissipates upon ejection [1,17]. The fluid mechanics during diastole, however, rely upon the asymmetry of the mitral valve orifice relative to the LV chamber [10,15]. During early diastolic filling, a strong clockwise vortex forms under the anterior mitral leaflet simultaneously with a weak counterclockwise vortex under the posterior mitral valve leaflet. During late diastole and isovolumic contraction, the weak counterclockwise vortex dissipates, while the anteriorly located strong vortex persists and grows, allowing for efficient blood streaming and minimization of intracardiac EL [10]. This process generates a kinetic energy reservoir, which can be utilized for ejection during systole, despite the relative increase in endocardial WSS [15,18]. Changes in either WSS or dissipative intracardiac energy, therefore, are indications of inappropriate vortex formation or dissipation during the cardiac cycle, pathologically increasing myocardial work.

Studies of VFM for elucidation of intraventricular flow patterns in HCM have demonstrated alterations in wall shear stress and energy dissipation compared to healthy adult and suggest that the altered flow patterns may contribute to disease [1,7,11,17]. In obstructive HCM, Ro et. al utilized VFM to analyze the mechanics of systolic anterior motion of the mitral valve [1]. They demonstrated variations of the angle of the mitral jet during diastole to be dependent on the presence of obstruction [1]. Furthermore, Ji

Table 3
Univariate correlations within Controls, HCM, and DCM (n = 85). Pearson Correlation between energetic parameters and other covariates.

	Age		BSA		HR (bpm)		Biplane EF (%)		CI (L/min/m^2)	
	r	p	r	p	r	p	r	p	r	p
Wall Shear Stress (WSS)										
Average WSS – Systolic (N/m^2)	−0.148	0.178	−0.093	0.398	0.136	0.216	0.101	0.359	−0.076	0.491
Average WSS – Diastolic (N/m^2)	**−0.383**	**0.0003**	**−0.438**	**< 0.0001**	**0.330**	**0.002**	**−0.381**	**0.0003**	0.209	0.055
Energy Loss (EL) – 3 Cycles										
Total EL (mW/m^3)	**−0.442**	**< 0.0001**	**−0.326**	**0.002**	**0.504**	**< 0.0001**	−0.018	0.871	**0.326**	**0.001**
Indexed Total EL (mW/m^2/m^3)	**−0.587**	**< 0.0001**	**−0.619**	**< 0.0001**	**0.607**	**< 0.0001**	−0.018	0.874	**0.326**	**0.002**
EL – Systolic (mW/m^3)	−0.210	0.054	−0.088	0.419	**0.358**	**0.001**	0.010	0.930	0.201	0.066
Indexed EL – Systolic (mW/m^2/m^3)	**−0.586**	**< 0.0001**	**−0.601**	**< 0.0001**	**0.638**	**< 0.0001**	−0.088	0.426	**0.317**	**0.003**
EL – Diastolic (mW/m^3)	**−0.469**	**< 0.0001**	**−0.404**	**0.0001**	**0.536**	**< 0.0001**	−0.024	0.830	**0.379**	**0.0003**
Indexed EL – Diastolic (mW/m^2/m^3)	**−0.523**	**< 0.0001**	**−0.565**	**< 0.0001**	**0.558**	**< 0.0001**	0.006	0.958	**0.289**	**0.007**
	E/A		**E/e'**		**LA Vol (mL/m^2)**		**GLS**		**GCS**	
	r	p	r	p	r	p	r	p	r	p
Wall Shear Stress (WSS)										
Average WSS – Systolic (N/m^2)	0.006	0.958	−0.116	0.289	−0.038	0.728	−0.096	0.381	−0.131	0.231
Average WSS – Diastolic (N/m^2)	**0.255**	**0.038**	0.213	0.050	−0.072	0.512	0.124	0.260	**0.325**	**0.002**
Energy Loss (EL) – 3 Cycles										
Total EL (mW/m^3)	0.053	0.627	**0.358**	**0.001**	0.106	0.336	0.070	0.524	−0.131	0.231
Indexed Total EL (mW/m^2/m^3)	−0.034	0.756	**0.363**	**0.001**	−0.081	0.464	0.002	0.983	−0.084	0.445
EL – Systolic (mW/m^3)	−0.174	0.112	**0.323**	**0.003**	**0.216**	**0.048**	0.165	0.131	−0.165	0.132
Indexed EL – Systolic (mW/m^2/m^3)	−0.141	0.198	**0.451**	**< 0.0001**	0.039	0.726	0.141	0.197	−0.061	0.577
EL – Diastolic (mW/m^3)	0.035	0.749	**0.325**	**0.002**	0.004	0.975	0.041	0.709	−0.088	0.420
Indexed EL – Diastolic (mW/m^2/m^3)	−0.049	0.306	**0.306**	**0.004**	−0.120	0.272	−0.025	0.822	−0.086	0.434

WSS – Wall Shear Stress, EL – Energy Loss.

et. al demonstrated that ventricular WSS is decreased during peak LV ejection in HCM, corresponding with significant flow alterations during late diastole and atrial systole [17]. In the same study, it was further demonstrated that the basilar vortex during isovolumetric contraction is absent in HCM [17]. In congruence with these results, our study has demonstrated significant changes in diastolic WSS, maximum systolic WSS, and indexed systolic EL. The hypertrophied ventricular wall and myocardial disarray result in an increase in ventricular stiffness, consequently increasing the energy expenditure during ventricular filling. As a result, the velocity associated with myocardial filling decreases, resulting in decreased momentum transfer to the ventricular wall and thus decreased wall stress. These changes are reflected by the significant decrease in diastolic WSS observed in our study. Our results demonstrated no change in WSS during systole as the decrease in ejection velocity associated with myocardial disarray is compensated for by the increase in contractility. Our study further demonstrated a significant increase in indexed systolic EL in HCM, likely due to the hypercontractile phenotype observed in HCM. Thus, changes in energetic parameters associated with HCM reflect the known changes in ventricular mechanics resulting from hypertrophy and myocardial disarray.

Few studies have been performed to assess ventricular fluid mechanics in DCM utilizing VFM [11,19,20]. Unlike in HCM, where vortex formation is absent due to EL during diastolic filling, vortex formation in DCM is present, but weakened and distorted. The mechanics observed in DCM utilizing VFM suggest that flow is reduced, resulting in local stagnation of blood flow and thrombus formation [11]. Similar findings have been observed in cases of systolic dysfunction secondary to ischemic injury [14,16]. Despite the observed systolic dysfunction in these patients, our results failed to resolve differences in energetic parameters between DCM and controls. We speculate that the altered kinetics of ventricular filling and ejection fail to result in significant elevations in WSS, as the elevated filling pressures themselves are insufficient to increase momentum transfer to the endocardium due to the increased surface area of the dilated ventricle. Based on these results, energetic parameters themselves fail to have the sensitivity and specificity to resolve the known changes in physiology in DCM compared to normal controls. We recognize that the observed results may be due to insufficient power, so future studies should aim to expand the sample size for identification of the clinical relevance of energetic parameters in the dilated LV. Additionally, future studies should aim to identify cutoffs for ventricular energetic parameters for relevant outcomes.

Significant correlations between all WSS and energetic parameters between HR, E/A. and E/e' were observed in our study. Additionally, multivariate regression of the same parameters yielded similar findings to univariate analysis. These data support previous studies assessing energetic parameters utilizing VFM in healthy adult left ventricles [9,10,12]. All WSS parameters and energetic parameters in our study were found to positively correlate with HR. Furthermore, we observed a significant correlation between EL parameters and E/e'. Multivariate regression demonstrated E/e' was one of few predictors of EL parameters. The E wave itself is a known predictor of systolic EL due to the Frank-Starling effect. In this schema, the E wave can be considered a measure of preload, and increased myocardial stretch is responsible for increased contractility, resulting in the observed increase in EL [10]. These findings are reflected in our study. Additionally, it is well known that systolic EL is known to correlate with LV fractional shortening [10]. Strikingly, our study observed no significant correlations between GLS and GCS. We hypothesize that the lack of correlation between ventricular strain and EL, despite the known relationship between strain and the strain energy function in mechanics, may suggest that EL parameters provide an alternative index of ventricular function, which is separate from subclinical myocardial dysfunction associated with impaired strain.

Despite the utility for quantification of intracardiac flow patterns in cardiomyopathy both here and in previous studies [1,21,22], clinical utility has been limited, particularly due to technological limitations. As discussed, VFM methods ignore the three-dimensional component of flow and solves the two-dimensional continuity equation. While 3D VFM implementations are possible, limitations in the acquisition frame rate hamper their clinical application [13,23,24]. Furthermore, inter and intra-operator variability is an issue [25]. Thus, while VFM methods provide a unique insight into intracardiac profiles in cardiomyopathy, further technological refinement is required.

4.1. Limitations

Our study has several limitations. Our study included small sample sizes in each of the cohorts. In our HCM cohort, we did not control for LV outflow tract obstruction (LVOTO). Systolic anterior motion of the mitral valve is known to change the filling angle of the mitral jet, which is subsequently deflected posteriorly by the enlarged septal bulge. Furthermore, during early systole, the velocity vector flow overlaps with the anatomic LVOT. As a result, obstruction is known to increase both systolic and diastolic EL. Lack of control for LVOTO may potentially elevate the observed EL in the HCM patients assessed in our study. Furthermore, we did not control functional mitral regurgitation (MR) in the DCM group, which is known to increase diastolic filling velocities and disrupt vortex formation. As a result, changes in diastolic EL may not accurately reflect the physiology in most cases of DCM without MR, which should be addressed in future studies. DCM itself is further not a case of pure systolic dysfunction, and the degree of diastolic dysfunction in DCM was not addressed in this study. In general, DCM and HCM are heterogeneous conditions. Consequently, there may be intrinsic variability within these groups not assessed in this study. Accordingly, correlations between ventricular energetics parameters and echocardiographic indices of diastolic function were weak. Furthermore, the two-dimensional simplification of the VFM methods may contribute to variance in the results. Future studies should therefore aim to correlate changes in ventricular energetics and WSS with specific genetic mutations in HCM and DCM, to better characterize the role of sarcomere dysfunction in abnormal ventricular energetics.

5. Conclusion

Recent interest in the role of ventricular EL and cardiovascular disease progression has increased the utilization of echocardiographic VFM in the investigation of cardiac pathophysiology. This study utilized VFM for assessment of systolic and diastolic ventricular WSS and intracardiac EL in HCM and DCM and correlated these data with traditional echocardiographic parameters. This study demonstrated significant elevation in diastolic WSS and indexed systolic EL in HCM. Significant, albeit weak, correlations of WSS and EL parameters between age, HR, E/A, and E/e' were observed. The changes in energetic parameters may represent novel indices of ventricular diastolic dysfunction. Future studies analyzing the relationships between ventricular energetic parameters and cardiovascular disease progression and outcomes are needed to further establish the clinical value of echocardiographic VFM.

Acknolwedgment

The authors acknowledge Hitachi Healthcare Americas for equipment support, Tom Wolk and Connie Casey BS, RDCS for technical assistance, Karl Stessy Bisselou Moukagna, MS for preliminary statistical analysis and Robert Spicer MD for subject recruitment support.

Appendix A. Supplementary material

Supplementary data to this article can be found online at https://doi.org/10.1016/j.ijcha.2020.100703.

References

[1] R. Ro, D. Halpern, D.J. Sahn, P. Homel, M. Arabadjian, C. Lopresto, M.V. Sherrid, Vector flow mapping in obstructive hypertrophic cardiomyopathy to assess the relationship of early systolic left ventricular flow and the mitral valve, J. Am. Coll. Cardiol. 64 (2014) 1984–1995.
[2] L. Xu, C. Sun, X. Zhu, W. Liu, S. Ta, D. Zhao, F. Wang, L. Liu, Characterization of left ventricle energy loss in healthy adults using vector flow mapping: Preliminary results, Echocardiography 34 (2017) 700–708.
[3] S.F. Nagueh, K.J. Middleton, H.A. Kopelen, W.A. Zoghbi, M.A. Quiñones, Doppler tissue imaging: a noninvasive technique for evaluation of left ventricular relaxation and estimation of filling pressures, J. Am. Coll. Cardiol. 30 (1997) 1527–1533.
[4] Y. Wang, R. Ma, G. Ding, D. Hou, Z. Li, L. Yin, M. Zhang, Left ventricular energy loss assessed by vector flow mapping in patients with prediabetes and type 2 diabetes mellitus, Ultrasound Med. Biol. 42 (2016) 1730–1740.
[5] T. Onishi, S.K. Saha, A. Delgado-Montero, D.R. Ludwig, T. Onishi, E.B. Schelbert, D. Schwartzman, J. Gorcsan III, Global longitudinal strain and global circumferential strain by speckle-tracking echocardiography and feature-tracking cardiac magnetic resonance imaging: comparison with left ventricular ejection fraction, J. Am. Soc. Echocardiogr. 28 (2015) 587–596.
[6] S.A. Reisner, P. Lysyansky, Y. Agmon, D. Mutlak, J. Lessick, Z. Friedman, Global longitudinal strain: a novel index of left ventricular systolic function, J. Am. Soc. Echocardiogr. 17 (2004) 630–633.
[7] K. Itatani, T. Okada, T. Uejima, T. Tanaka, M. Ono, K. Miyaji, K. Takenaka, Intraventricular flow velocity vector visualization based on the continuity equation and measurements of vorticity and wall shear stress, Jpn. J. Appl. Phys. 52 (2013) 07HF16.
[8] Y. Zhong, W. Zhu, C.-M. Li, L. Rao, Assessment of cardiac dysfunction by dissipative energy loss derived from vector flow mapping, J. Cardiol. 67 (2016) 122.
[9] T. Honda, K. Itatani, M. Takanashi, A. Kitagawa, H. Ando, S. Kimura, N. Oka, K. Miyaji, M. Ishii, Exploring energy loss by vector flow mapping in children with ventricular septal defect: pathophysiologic significance, Int. J. Cardiol. 244 (2017) 143–150.
[10] K. Akiyama, S. Maeda, T. Matsuyama, A. Kainuma, M. Ishii, Y. Naito, M. Kinoshita, S. Hamaoka, H. Kato, Y. Nakajima, Vector flow mapping analysis of left ventricular energetic performance in healthy adult volunteers, BMC Cardiovasc. Disord. 17 (2017) 21.
[11] G. Pedrizzetti, G. La Canna, O. Alfieri, G. Tonti, The vortex—an early predictor of cardiovascular outcome?, Nat. Rev. Cardiol. 11 (2014) 545.
[12] T. Hayashi, K. Itatani, R. Inuzuka, N. Shimizu, T. Shindo, Y. Hirata, K. Miyaji, Dissipative energy loss within the left ventricle detected by vector flow mapping in children: Normal values and effects of age and heart rate, J. Cardiol. 66 (2015) 403–410.
[13] P.P. Sengupta, G. Pedrizzetti, P.J. Kilner, A. Kheradvar, T. Ebbers, G. Tonti, A.G. Fraser, J. Narula, Emerging trends in CV flow visualization, JACC Cardiovasc. Imaging. 5 (2012) 305–316.
[14] J. Lu, W. Li, Y. Zhong, A. Luo, S. Xie, L. Yin, Intuitive visualization and quantification of intraventricular convection in acute ischemic left ventricular failure during early diastole using color Doppler-based echocardiographic vector flow mapping, Int. J. Cardiovasc. Imaging. 28 (2012) 1035–1047.
[15] H. Zhang, J. Zhang, X. Zhu, L. Chen, L. Liu, Y. Duan, M. Yu, X. Zhou, T. Zhu, M. Zhu, The left ventricular intracavitary vortex during the isovolumic contraction period as detected by vector flow mapping, Echocardiography. 29 (2012) 579–587.
[16] H. Zhang, L. Liu, L. Chen, N. Ma, L. Zhou, Y. Liu, Z. Li, C. Liu, R. Hou, S. Zhu, The evolution of intraventricular vortex during ejection studied by using vector flow mapping, Echocardiography 30 (2013) 27–36.
[17] L. Ji, W. Hu, Y. Yong, H. Wu, L. Zhou, D. Xu, Left ventricular energy loss and wall shear stress assessed by vector flow mapping in patients with hypertrophic cardiomyopathy, Int. J. Cardiovasc. Imaging 34 (2018) 1383–1391.
[18] R. Chen, B. Zhao, B. Wang, H. Tang, P. Li, M. Pan, L. Xu, Assessment of left ventricular hemodynamics and function of patients with uremia by vortex formation using vector flow mapping, Echocardiography. 29 (2012) 1081–1090.
[19] Q. Li, L. Huang, N. Ma, Z. Li, Y. Han, L. Wu, X. Zhang, Y. Li, H. Zhang, Relationship between left ventricular vortex and preejectional flow velocity during isovolumic contraction studied by using vector flow mapping, Echocardiography 36 (2019) 558–566.
[20] Y. Han, L. Huang, Z. Li, N. Ma, Q. Li, Y. Li, L. Wu, X. Zhang, X. Wu, X. Che, Relationship between left ventricular isovolumic relaxation flow patterns and mitral inflow patterns studied by using vector flow mapping, Sci. Rep. 9 (2019) 1–8.
[21] T. Honda, K. Itatani, K. Miyaji, M. Ishii, Assessment of the vortex flow in the post-stenotic dilatation above the pulmonary valve stenosis in an infant using echocardiography vector flow mapping, Eur. Heart J. 35 (2014) 306.
[22] A. Vitarelli, F. Martino, L. Capotosto, E. Martino, C. Colantoni, R. Ashurov, S. Ricci, Y. Conde, F. Maramao, M. Vitarelli, S. De Chiara, C. Zanoni, Early Myocardial Deformation Changes in Hypercholesterolemic and Obese Children and Adolescents: A 2D and 3D Speckle Tracking Echocardiography Study, Medicine (Baltimore) 93 (2014). https://journals.lww.com/md-journal/Fulltext/2014/09020/Early_Myocardial_Deformation_Changes_in.4.aspx.
[23] A. Falahatpisheh, G. Pedrizzetti, A. Kheradvar, Three-dimensional reconstruction of cardiac flows based on multi-planar velocity fields, Exp. Fluids 55 (2014) 1848.
[24] A. Falahatpisheh, A. Kheradvar, A framework for synthetic validation of 3D echocardiographic particle image velocimetry, Meccanica 52 (2017) 555–561.
[25] A. Kheradvar, On the accuracy of intracardiac flow velocimetry methods, (2017).